Natural Resources for Human Health

eISSN: 2583-1194

Original Research

Received 22 July 2026
Revised 18 Aug 2026
Accepted 05 Sep 2026

Natural Resources for Human Health 2026, Vol. 6 (20s): 79–91

KEYWORDS:
Pennisetum glaucum, Spectroscopy, Thermogravimetric, Biodegradation

Extraction and Characterisation of Cellulose derived from Pearl Millet (Pennisetum glaucum) Waste for Sustainable Biomedical Applications

Ajesh Chauhan[1], Rishabha Malviya*[1]

[1]Department of Pharmacy, School of Medical and Allied Sciences, Galgotias University, Greater Noida, Uttar Pradesh, India

ABSTRACT: The residue of pearl millet (Pennisetum glaucum L., family: Poaceae) production, widely utilised in agriculture, has high potential as a sustainable resource for scientific development of new generative materials. The stalks and husks of Pennisetum glaucum (Pearl millet or Bajra) consist mostly of cellulose content. The primary objective of this research was to extract and characterise cellulose from agricultural residue of pearl millet. The extraction of cellulose was performed via a microwave-assisted green extraction method, the extracted cellulose was further characterised through various techniques, including Fourier Transform Infrared Spectroscopy (FTIR), Thermogravimetric Analysis (TGA), X-ray Diffraction (XRD), Differential Scanning Calorimetry (DSC), Scanning Electron Microscopy (SEM), ash value determination, contact angle measurement, swelling index assessment, moisture content analysis, chemical resistance evaluation, and biodegradability testing by burial method. The cellulose was effectively isolated by green extraction method along with alkali treatment followed by bleaching and characterised using several analytical techniques. The organoleptic assessment indicated that the cellulose possessed a fibrous texture, a colour from pale cream to light yellow, and an odourless. FTIR spectroscopy shows the efficient removal of the majority of non-cellulosic components and verified the presence of distinctive cellulose functional groups. The DSC analysis identified an apparent endothermic transition, demonstrating the thermal resistance of the extracted cellulose, while the TGA demonstrated considerable thermal stability, with primary degradation occurring at high temperatures. The coarse, porous, and fibrillated surface morphology, as illustrated the SEM micrographs, enhanced the surface area and adsorption capacity. An XRD analysis found significant diffraction peaks at 2θ values of around 16°, 22°, and 34°, confirming the formation of a highly crystalline cellulose structure. Crystalline structure abundant in polysaccharides was shown by solid-state 13C NMR spectra, which showed distinct resonances in the 60-110 ppm region. The results of the contact angle measurements showed that the surface was quite hydrophilic, which is a good indicator of its wettability. The cellulose's high purity and stability were demonstrated by its acceptable moisture content and low ash level. The ability to absorb water was demonstrated in swelling tests in acidic, phosphate buffer, and pure water settings. Chemical resistance studies found almost no degradation in acidic, buffered, and water-based conditions. The material's eco-friendliness and biodegradability were confirmed by the biodegradability study, which showed a steady weight drop over 21 days. The structural, thermal, physicochemical, and biodegradation properties of pearl millet-derived cellulose were promising for pharmaceutical, biomedical, packaging, and environmental applications as a sustainable and cost-effective biomaterial.

1. INTRODUCTION

Petrochemical based plastics, including Poly Ethyl Terephthalate (PET), Poly Butylene Terephthalate (PBT), Polypropylene (PP), Polystyrene (PS), and Polyvinyl Chloride (PVC), are extensively utilised in daily life due to their versatility, affordability, lightweight nature, and superior thermal qualities [1]. Plastics are utilised to manufacture items such as water bottles, coffee

cups, cutlery, and grocery bags. Petrochemical-based polymers are not environmentally sustainable due to their significant carbon footprint. Attributes such as cost-effectiveness, durability, and lightweight nature render plastics significantly more advantageous than metals, wood, paper, and similar materials. They are beneficial in nearly all industrial sectors. The overutilization of plastics has inflicted significant harm on the environment, with an estimated annual production of approximately 34 millon tonnes of plastics by humans. Only 7% is recycled, while the remaining 93% is disposed of in landfills, oceans, and seas [2,3]. In 2015, about 300 million tonnes of plastic were utilised globally. The incineration of plastic releases numerous hazardous emissions, including carbon dioxide and methane, which are greenhouse gases that impact the global climate. Petrochemical-based goods contribute to numerous issues, including the accumulation of trash in terrestrial environments and natural habitats such as seas and oceans. Plastic pollution is causing disruptions in thyroid hormone levels in humans [4]. The incorporation of chemical compounds in plastic manufacture renders them hazardous and carcinogenic. Initiatives to diminish plastic usage have transpired in various domains, hence enhancing plastic recycling efforts. Additives like phthalate plasticisers and brominated flame retardants are utilised in plastic manufacturing. Plasticisers are compounds used into plastics to enhance its flexibility, durability, clarity, and longevity. Consequently, scientists are currently exploring more alternate solutions [5,6].

Bioplastics are biodegradable polymers derived from renewable resources. Renewable sources include potato starch, corn starch, fibres derived from pineapple, jute, pearl millet, corn, hemp, banana stems, cassava, newspaper pulp, waste paper, Prosopis juliflora, citrus waste, cyanobacteria, Pseudomonas putida, and Bacillus sp. The use of innovative processes for bioplastic production that foster sustainable solutions and diminish plastic waste has been significantly promoted in recent years [7]. Pearl millet is a significant source of cellulose; however, cellulose derived from potato, wheat, rice, barley and oat are also being utilised. Bio-based polymers can be decomposed by algae, fungi, and bacteria. These polymers are innovative materials of the 21st century and hold significant importance. Currently utilised as packaging materials, these will be employed in the production of numerous products, including electronics and automotive components, in the future [8].

The need for eco-friendly substitutes made from renewable agricultural resources has increased in response to growing environmental concerns associated with synthetic and non-biodegradable materials. A major grain crop grown in dry and semi-arid regions, pearl millet (Pennisetum glaucum) is mainly used for human consumption and animal feed. As an agricultural residue, pearl millet stalks and husks remain after harvest in large quantities, and they are often burnt or disposed of, worsening environmental contamination. Sustainable biomaterials can be made from these agricultural by-products, which are a rich and untapped source of cellulose. Sustainable and environmentally friendly processing techniques can efficiently recover the high cellulose content found in pearl millet wastes. A wide range of analytical techniques can be used to study the isolated cellulose in detail. These include FTIR, DSC, TGA, SEM, NMR, XRD, contact angle measurement, moisture content assessment, ash value analysis, swelling index determination, chemical resistance evaluations, and many more. Agricultural waste from pearl millet can be used to extract cellulose, which improves waste management and decreases pollution. This renewable raw material can then be used to make materials that are biodegradable, sustainable, and have high performance. These materials can be used in the pharmaceutical, packaging, biomedical, and environmental industries.

2. MATERIALS AND METHODS

2.1 Study Material

The chemicals used in the research were toluene, hydrogen peroxide, hydrochloric acid, ethanol, and sodium hydroxide.

2.2 Sample Collection

The pearl millet plants were obtained from agricultural farms located in Sonipat, Haryana (28.8971° N, 77.1920° E). Additionally, the plant was authenticated by Dr. Sandeep Chauhan, Scientist F & In-charge, BGIR Noida from the Ministry of Environment, Forest and Climate Change, Botanical Survey of India, Botanic Garden of Indian Republic, Sector 38A, Gautam Budh Nagar, Noida-201303, with authentication reference number as "BSI/BGIR/1/TECH./2025/223."

2.3 Extraction Procedure

The pearl millet stalks, an extensively available agricultural byproduct, possesses considerable potential as it can be utilised as a sustainable biomaterial. This research investigates the efficient extraction and thorough characterisation of pearl millet stem cellulose. The extraction process comprised a series of steps including de-waxing, alkali treatment, and bleaching, which

effectively eliminated lignin, hemicellulose, waxes, and other non-cellulosic constituents, resulting in efficient extraction of cellulose. The pearl millet stem were thoroughly dried, and the biomaterial was removed from the pearl millet stem. The obtained biomaterial was then subjected to de-waxing using a binary solvent system containing ethanol and toluene in a ratio of 2:1. The de-waxing process was conducted utilising a soxhlet apparatus for a duration of 4 h at 60 to 70° C temperature range [9]. After the de-waxing, the material was subjected to alkaline treatment utilising a 5% (w/v) sodium hydroxide solution, at a temperature of 50 °C for a duration of 2 hours. The alkali treatment was conducted to remove hemicellulose and lignin [10]. Subsequently, the material was allowed to cool to normal temperature and underwent multiple washings with distilled water.

Furthermore, the material was subjected to bleaching for de-colouration. The bleaching was performed using the bleaching solution of hydrogen peroxide with distilled water in the ratio of 3:10 (v/v) [11]. After bleaching, the material was allowed to cool to normal temperature and underwent multiple washings with distilled water. Furthermore, the neutralised cellulose was thoroughly dried in the hot air oven. (Figure 1) shows the extraction procedure of pearl millet stem cellulose. The extracted cellulose biomaterial was then further processed to various characterisation parameters [12]



Figure 1: Diagrammatic representation of Pearl millet cellulose extraction procedure: (1) solvent dewaxing using soxhelt (2) alkali treatment with NaOH (3) thorough washing, (4,5) H_2O_2 bleaching, final washing and drying, and (6) Obtained Cellulose.

2.4 Analytical Methods

The extracted cellulose from the Pearl millet was characterised using several parameters, including FTIR, SEM, TGA, DSC, XRD, contact angle measurement, ash value, swelling index, moisture content, chemical resistance, and biodegradability tests.

2.4.1. Organoleptic Properties

The organoleptic assessment of corn cob cellulose was performed to evaluate its colour, physical characteristics, and odour.

2.4.2. Fourier transform infrared spectroscopy (FTIR)

Fourier transform infrared spectroscopy (FTIR) was conducted to ascertain and identify the principal chemical functional groups in the extracted cellulose utilising the Bruker FTIR Alpha II instrument. The cellulose sample was examined within the range of 4000–400 cm^{-1}, and the spectra were documented.

2.4.3 Thermogravimetric analysis (TGA)

Pearl Millet Cellulose thermogravimetric analysis (TGA) was carried out to determine thermal stability, measure volatile component fractions, and examine mass variations with respect to temperature., the thermogravimetric analysis was carried out by using Mettler Toledo TGA/DSC 3+ system. Temperatures ranging from 30 to 600°C were applied to the sample in a nitrogen environment at a controlled pace of 10°C per minute.

2.4.4. Differential scanning calorimetry (DSC)

The cellulose from Pearl Millet performed differential scanning calorimetry (DSC) to evaluate the temperature-dependent variations in enthalpy (heat flow). The Mettler Toledo TGA/DSC 3+ apparatus was employed to perform Differential Scanning Calorimetry (DSC). The sample underwent heating in a nitrogen environment at a controlled pace of 10°C per minute, with the temperature ranging from 30°C to 600°C. The DSC curves were generated and analysed.

2.4.5. Morphological Characterisation:

Scanning electron microscopy (SEM) was conducted for the visualisation and micro-structural investigation of cellulose. The scanning electron microscopy was conducted using a JEOL JSM-7610F Plus SEM equipment. The sample was coated with gold and analysed under high vacuum conditions. The cellulose was observed at a magnification of 2500x.

2.4.6. X-ray diffraction (XRD)

To determine how crystallin the cellulose was in the sample, X-ray diffraction (XRD) was used. Utilising a Bruker D8 Advance X-ray Diffractometer, the material was subjected to X-ray diffraction (XRD) examination. The sample was examined using Cu Kα radiation (λ = 1.5406 Å) within the 2θ range of 5° to 40°.

2.4.7. Contact angle

To determine if the cellulose was hydrophobic or hydrophilic, the contact angle test was performed. The contact angle was measured using a Rame Goniometer model 100-00-230. The results were presented as the average of three measurements accompanied by standard deviations.

2.4.8. Moisture Content

The moisture content of the sample was ascertained by quantifying the weight of water contained inside the cellulose. The moisture content was evaluated by determining the initial mass (W_1) of the sample, which was subjected to drying in a hot air oven at 105 ± 2°C for 24 hours. The dried sample was thereafter permitted to cool in a desiccator, after which the weight was measured again (W_2) [13]. The moisture content was determined using Equation 1. The data was reported as the mean of triple measurements accompanied with standard deviations.

$$\text{Moisture Content}(\%) = (\text{Initial weight} - \text{Final weight}/\text{Initial weight}) \times 100 \quad \text{Equation 1}$$

2.4.9. Ash Value

The ash value refers to the quantity of non-combustible inorganic residue that persists following the incineration of a cellulose sample. This value denotes the mineral composition and purity of the sample. Ash content refers to the quantity of inorganic residue remaining post-combustion. The ash value of the cellulose was ascertained by incinerating a pre-weighed sample in a crucible at elevated temperatures, followed by weighing the residual ash.The sample was accurately measured at 100 mg. After that, the sample was muffle-furnaced and burnt in the crucible for a few minutes at about 500°C. To prevent moisture absorption, the crucible was carefully cooled in a desiccator after ashing, and the cellulose ash's weight was again recorded [14]. We present the results as the mean of three measurements with standard deviation for the ash content, which was determined using Equation 2.

$$\text{Ash Value } (\%) = (\text{Weight of ash}/\text{weight of dry Fibre}) \times 100 \quad \text{Equation 2}$$

2.4.10. Swelling index

Cellulose's swelling capacity in three different liquid solvents (distilled water, 0.1 N HCl, and a phosphate buffer at pH 7.4) was determined using the swelling index. Distilled water was used to immerse a pre-weighed specimen (W_1) for a duration of 24 hours. We reweighed the sample (W_2) after 24 hours and removed the excess liquid. Equation 3 was used to determine the swelling index. With the standard deviation included, the findings were given as the mean of three separate measurements [15].

$$\%\ \text{Swelling} = (Ws - Wd/Wd) \times 100 \quad \text{Equation 3}$$

Where:

Ws:- Swollen weight of cellulose in (g)

Wd:- Dried weight of the cellulose in (g)

2.4.11. Chemical Resistance Test

One way to determine cellulose's chemical resistance was to see if its weight changed after being exposed to certain chemical solutions (distilled water, phosphate buffer, and HCl solution). Fifty milligrams of the cellulose sample was immersed in three separate solutions for 24 hours to determine its stability under acidic, physiological, and neutral conditions in order to evaluate chemical resistance: distilled water, a pH 7.4 phosphate buffer, and 0.1 N hydrochloric acid. A hot air oven was used to dry the samples after 24 hours of removing extra liquid. The specimens' mass was recorded after complete drying [16]. Afterwards, we used Equation 4 to evaluate the chemical resistance. With standard deviations included, the data were given as the mean of three separate measurements.

Weight Remaining=(Initial weight-Final dried weight/Final dried weight)×100 Equation 4

2.4.12. Biodegradability

Soil burial biodegradability testing measures the rate of sample breakdown in the presence of soil by tracking changes in mechanical properties and mass loss; this test was used to evaluate the biodegradability of the cellulose sample. The study utilised a 200 mL plastic container filled with 200 g of compost sourced from agricultural land in Sonipat, Haryana, India. A 0.1 g sample of cellulose was positioned in a container at a depth of 5 cm. To preserve moisture, 5 cc of water was introduced to the container every 24 hours [17,18]. A little drainage outlet was constructed at the base of the container to facilitate the expulsion of surplus water. The biodegradability assessment was performed at ambient room temperature. After 21 days, the sample was extracted from the container and subsequently rinsed with distilled water. Thereafter, the sample was dried and subsequently weighed. The assessment of biodegradability was performed by determining the percentage of weight loss, utilising equation 5. The data were expressed as the mean of three measurements, together with the standard deviation.

Weight loss%=(Initial weight Final weight/Final weight)×100 Equation 5

3. RESULTS AND DISCUSSION

Pearl millet straw that has been treated and PMC was obtained has a texture that is soft, fibrous, and flicks, and it has a white-brown overall appearance. It is odourless.

3.1 FTIR Interpretation of Pearl Millet Cellulose

The FTIR spectrum of cellulose isolated from pearl millet exhibits the characteristic absorption bands corresponding to the polysaccharide backbone and hydroxyl-rich structure of cellulose. The major peaks observed in the spectrum confirm the successful extraction and purification of cellulose material. The presence of intramolecular and intermolecular hydrogen-bonded hydroxyl groups in cellulose is responsible for the broad absorption band that appears between 3300 and 3400 cm^{-1}. The hydrophilic nature of cellulose is indicated by this broad peak, which is characteristic of lignocellulosic materials. In the cellulose structure, the C-H stretching vibrations of aliphatic methylene (-CH_2) groups are responsible for the peak near 2900 cm^{-2}. This proves that polysaccharide chains are present. The adsorbed water molecules linked to cellulose, as a result of its hygroscopic behaviour, could be attributed to a faint band at approximately 1640 cm^{-1}. The presence or weakening of peaks around 1730 cm^{-1} suggests that the hemicellulose and waxy ester components were successfully extracted. Crystalline cellulose areas are characterised by absorption peaks between 1420 and 1370 cm^{-1}, which are linked to CH_2 bending and C-H deformation vibrations. O-H bending and C-O stretching vibrations, which correlate to the band around 1315-1240 cm^{-1}, indicate that there are cellulose ether and alcohol functionalities. The C-O-C glycosidic bridge stretching and C-O stretching vibrations of the pyranose ring structure in cellulose are responsible for a strong and noticeable absorption region reported about 1160-1030 cm^{-1}. The presence of these peaks provides further evidence that the recovered substance is polysaccharide. The β-glycosidic bond, which is a fingerprint peak of cellulose, is represented by the peak near 895 cm^{-1}. It is a coupling between glucose units. All things considered, the FTIR spectrum proves that the extracted pearl millet biomass is primarily composed of cellulose and shows that non-cellulosic contaminants including lignin and hemicellulose were heavily removed throughout the purification procedure. Previous research, it was found that the FTIR analysis of Pearl millet biomaterial produced similar results. Pavas et al. demonstrate that N-H and C-H compounds exhibits peaks between1800 to 800 cm-1.

Pearl millet has a prominent absorption at 3269 cm-1 due to O-H bond stretching, along with additional peaks at 1645 and 1542 cm-1 associated to N-H bond stretching [19].

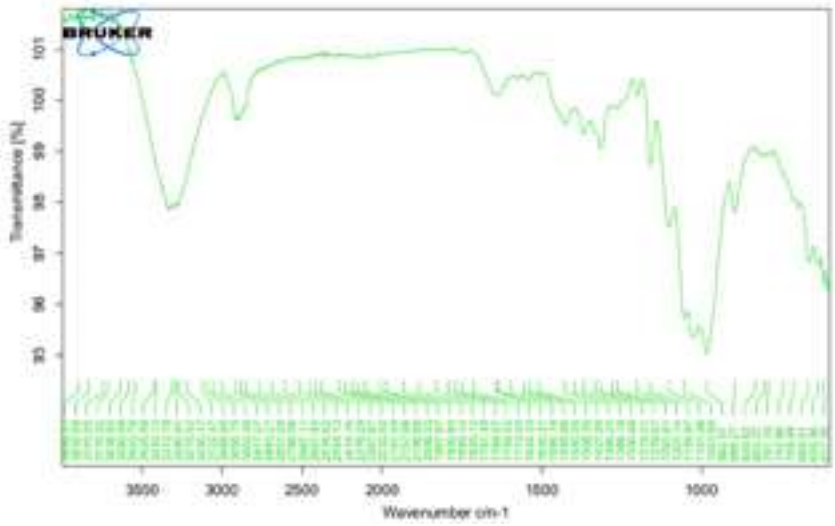


Figure 2. FTIR spectroscopy of pearl millet cellulose

Table 1. FTIR spectroscopy of pearl millet cellulose

S.no	Wavenumber	Group	Remarks
1	3313cm^{-1}	O-H stretching	Presence of Phenols, Alcohols, Absorbed moisture, Cellulose materials (Natural fibre)
2	3089 cm^{-1}	=C-H stretching	Indicates aromatic C–H vibration of lignin or unsaturated compounds.
2	2943 cm^{-1}	C-H stretching (Aliphatic)	Presence of -CH2 and -CH3 groups Reduced intensity after dewaxing confirms removal of waxy substances. Long hydrocarbon chain
5	2902 cm^{-1}	C–H stretching	Presence of cellulose backbone
3	1713 cm^{-1}	C=O stretching	Presence of Ester groups, Hemicellulose, wax and Fatty acids. Decreased intensity confirming effective dewaxing.
4	1635 cm^{-1}	H-O-H bending C=C stretching	Presence of bound water Aromatic rings vibration, lignin present
5	1508 cm^{-1}	Aromatic skeletal vibration	Ligin content
6	1427 cm^{-1}	CH2 Bending	Characteristic cellulose peak
7	1368 cm^{-1}	C-H Bending	Polisaccaride Backbone

8	1262 cm^{-1}	C-O Stretching	lignin/hemicellulose
9	1159 cm^{-1}	C-O-C Stretching C-O Stretching	Polisaccaride (Cellulose)
10	896 cm^{-1}	Beta glycosidic linkage	Cellulose backbone Confirms Beta 1-4 linkage structure

3.2 TGA/DSC of Pearl Millet Cellulose

The thermal properties of pearl millet cellulose were evaluated via thermogravimetric analysis (TGA) and differential scanning calorimetry (DSC). The obtained thermogram demonstrate that cellulose materials Shows thermal stability and display a characteristic degradation pattern. The initially observed slight weight loss in the TGA curve below 120°C is due to the evaporation of physically adsorbed moisture and volatile components in the extracted cellulose sample. The hygroscopic properties of cellulose, due to its many hydroxyl groups, are demonstrated by initial mass reduction. The thermal degradation of the cellulose backbone was shown by a significant degradation phase occurring between 300°C and 380°C. The thermogram demonstrates a significant weight loss of around 57.22%, indicating depolymerisation and the destruction of glycosidic linkages in the cellulose structure. At this phase, the cellulose chains primarily decompose into levoglucosan, carbon dioxide, and char residues, along with various volatile byproducts. The isolated cellulose demonstrated notable thermal stability, with an onset degradation temperature of approximately 314.03°C and a maximum degradation temperature (Tmax) of roughly 353.34°C. Crystalline cellulose domains were seen, but amorphous non-cellulosic impurities such as lignin including hemicellulose were successfully eliminated during extraction, as evidenced by the comparatively elevated degradation temperature. The formation of carbonaceous char and inorganic mineral constituents may have contributed to the residual mass of around 0.506 mg, or nearly 32.90% of the initial mass following thermal breakdown. The thermal decomposition behaviour observed in TGA is validated by the DSC thermogram. The evaporation of moisture is occurs during an endothermic transition at lower temperatures, whereas the cleavage and fragmentation of cellulose chains are indicated by the significant thermal event at the degradation zone. The reduced concentrations of hemicellulose and lignin, along with a significant lack of degradation peaks, indicates a relatively pure form of cellulose. Rapid pyrolysis of cellulose, hemicellulose, and lignin at temperatures between 250 to 380 °C results in the generation of volatile compounds, including water, carbon monoxide, and carbon dioxide, in addition various organic compounds, as evidenced by the mass reduction noted within this temperature range (Costa F et al., 2019) [20].

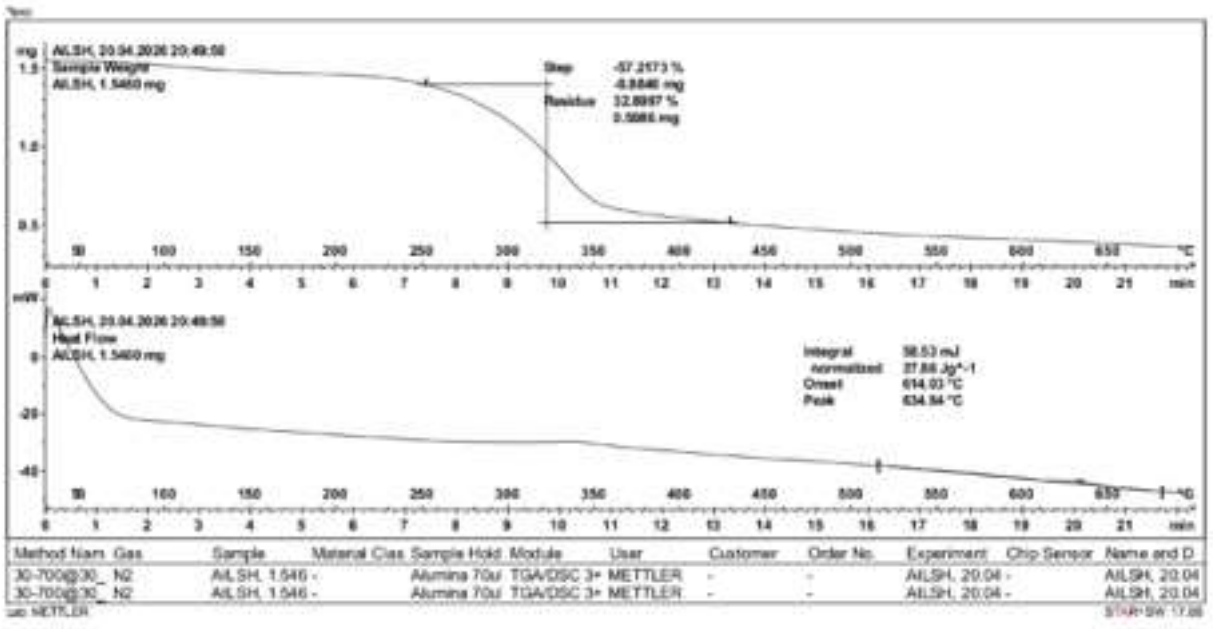


Figure 3: TGA and DSC analysis of Pearl Millet cellulose.

3.3. SEM Interpretation of Pearl Millet Cellulose

The surface morphology of pearl millet cellulose was analysed by using scanning electron microscopy (SEM). The distinct fibrous and asymmetrical structure of cellulose is illustrated in the scanning electron micrograph, obtained at approximately 2500× magnification with a 10 μm scale bar. The image depicts irregular particle aggregation defined by fibrillar formations that are rough, flaky, and sheet-like. The chemical extraction process probably eliminated amorphous components such as hemicellulose, lignin, waxes, and other non-cellulosic impurities, resulting in cellulose fibres characterised by a non-uniform and porous surface morphology. The observed layered and fractured surface structure signifies partial defibrillation and rupture of the dense lignocellulosic matrix, leading to the exposure of cellulose microfibrils. The morphological changes validates the efficacy of the alkali and bleaching treatments employed to remove cellulose from pearl millet biomass. The SEM image further demonstrate that the extracted cellulose exhibits an increased surface area and improved porosity, due to the presence of fractures, cavities, and inter-fibrillar gaps. The structural features facilitate several applications, such as the development of biodegradable materials, adsorption, drug loading, and polymer reinforcement. The lack of smooth, compact, and highly rigid structures signifies a substantial removal of lignin and hemicellulose components, resulting in a comparatively purified cellulose substance. The rough surface texture further substantiates that the cellulose chains are extensively hydrogen-bonded to each other.

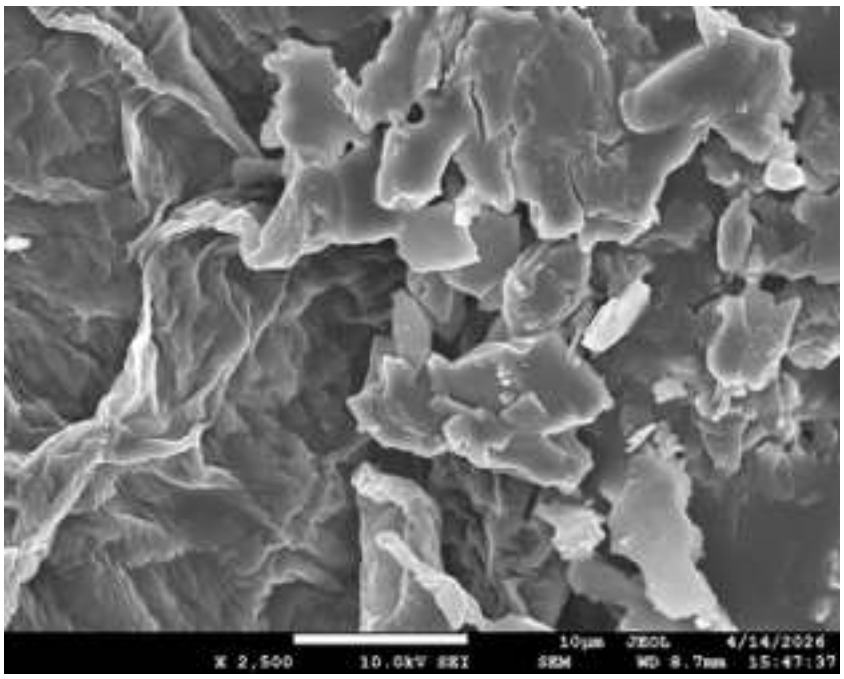


Figure 4: SEM analysis of pearl millet cellulose.

3.4. X-ray diffraction (XRD):

The crystalline structure of the isolated cellulose was analysed by X-ray diffraction (XRD), and the resulting diffraction pattern is illustrated in (Figure 5). The diffractogram displayed several sharp and significant diffraction peaks, indicating that the extracted material is mostly crystalline. The sharp and narrow diffraction peaks indicates the presence of well-ordered crystalline domains, while the absence of a substantial broad amorphous halo implies that the quantity of amorphous material is negligible. The diffraction profile showed a sequence of distinct reflections in the low- and medium-angle ranges (about 10–40° 2θ), signifying the presence of well-ordered crystalline planes. The narrow full width at half maximum (FWHM) of the primary diffraction peaks indicates exceptional crystallinity and comparatively large crystallite domains. Weak diffraction peaks detected at increased diffraction angles (about 65–80° 2θ) correlate to higher order lattice reflections, thereby confirming the structural integrity of the crystalline phase. The presence of many diffraction peaks in the diffractogram signifies that the sample is polycrystalline and may contain various crystalline phases. In lignocellulosic materials, additional diffraction peaks are often attributed to residual inorganic components, such as silica, calcium, potassium, and magnesium ions naturally present in agricultural biomass. Residual mineral phases may continue despite chemical purification, depending on the extraction conditions. The diffraction properties of cellulose extracted from pearl millet biomass indicate that the extraction technique effectively removed a significant quantity of amorphous components, such as lignin and hemicellulose, while preserving the structure of the organised cellulose microfibrils. The improvement in crystallinity results from the celebrated elimination of non-crystalline constituents during alkali and bleaching treatments, hence enhancing the accessibility of crystalline cellulose regions.The enhanced crystallinity observed in this analysis is expected to improve the thermal stability, mechanical strength, and dimensional stability of the extracted cellulose. Likewise, the XRD patterns observed in the study by Qi-Yuan Chen et.al. revealed that the PVP and Ag-NPs/PVP samples had 2θ peaks at around 22°. In the Ag-NPs/PVP curve, the diffraction peaks at 2θ = 38°, 44°, 64.3°, and 77.3° represent the face centred cubic (FCC) silver planes (111), (200), and (220), respectively. In agreement with the observed size range of silver nanoparticles (13-28 nm) by TEM, the average crystal size of Ag-NPs, as determined by the Scherrer formula, was 14.88 nm. The findings of the investigation demonstrate that the PVP-protected, tiny Ag-NPs are stable in a DMAc solution [21].

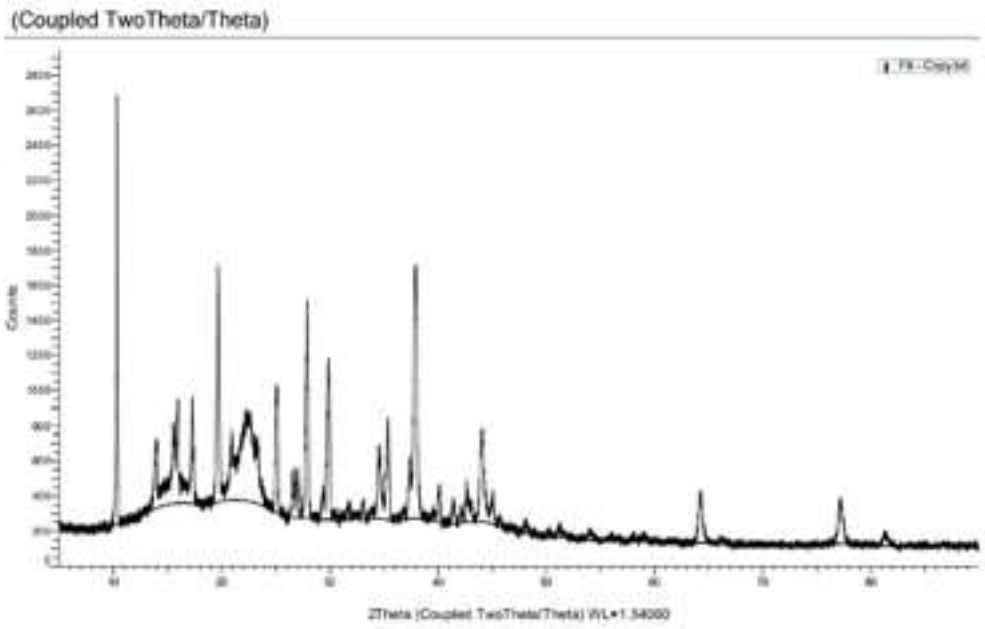


Figure 5: XRD analysis of pearl millet cellulose.

3.5 Contact Angle

The contact angle of the pearl millet cellulose was found to be 66.83°, 70.77°, and 68.82°. The mean value of the contact angle of the cellulose is 68.80° (Table 2). As the contact angle is calculated to determine the hydrophobic and hydrophilic characteristics of a surface. A contact angle measuring below 90° denotes hydrophilicity in the sample, whereas an angle above 90° indicates hydrophobic characteristics. The measurement of the contact angle, approximately 68.80°, depicted the pearl millet cellulose as hydrophilic in nature, indicating its capacity for water interaction while preserving structural integrity. As a result, the hydrophilic properties of the pearl millet cellulose were established. Previous research has found this trait to be true.

Similar wettability characteristics have been demonstrated by a variety of lignocellulosic fibres Water contact angles ranging from 40 to 50 degrees were seen in hemp, curaua, fique, jute, piassava, pineapple, ramie, and sisal fibres, as reported by Schellbach et al. [22]. This indicates that the surface qualities of these fibres are produced by cellulose-rich hydroxyl groups, which are weakly hydrophilic.

3.6. Moisture Content

The oven-drying method was used to assess the moisture content of pearl millet cellulose for 24 hours at a temperature of 105 ± 2°C (Table 2). The weight loss investigation found that the cellulose from pearl millet contains 3% moisture. So, there's no need to worry about the cellulose degrading or growing microbes because it stays stable and can be processed further. Verification of post-extraction stability and resistance to microbiological degradation was provided by the determination of moisture content, which was around 3%. Previous research has found this trait to be true. For example, Balasubramanian S. et. al. found the moisture content of the pearl millet based biomaterial to 4.5% [23].

3.7 Ash Value

The ash value of the sample was found to be 12.0 % ±1.3 %, indicating a significant presence of inorganic residues post-combustion (Table 2). Minerals, which are usually kept after biomass is thermally degraded, are indicated by this value as being present in the sample. Pearl millet cellulose might be considered an appropriate biomaterial with the properties of a solid biomaterial due to its low ash value [24].

3.9. Swelling Index

In distilled water, the swelling index of Pearl millet cellulose was 110%; in a phosphate buffer with a pH of 7.4 it was 157.5%; and in hydrochloric acid it was 240%. The cellulose fibres absorb moderate amounts of water in distilled water, as shown by

the swelling index of 110%. Hydrogen bonding with water molecules is made easier by the abundance of hydroxyl (-OH) groups in cellulose, which is primarily responsible for this characteristic. Nevertheless, the total swelling capacity is limited due to the compact arrangement of crystalline cellulose domains, which prevents water from penetrating the polymeric network extensively. In phosphate buffer (pH 7.4), the swelling index was 157.5%, which is relatively higher. Somewhat ionised surface functional groups and increased intracellular osmotic pressure within the cellulose matrix might explain why there's an increase in swelling in buffer solution. It is possible that the buffer ions reduce the strength of the intermolecular hydrogen bonds in the cellulose chains, which will cause the fibrillar structure to relax and enhance the passage of water into the polymer network. Anecdotal evidence suggests that plant-derived cellulose materials, which undergo increased hydration and structural relaxation under physiological pH values, swell more than other materials. The interaction between solvent ions and cellulose hydroxyl groups causes acidic and ionic environments to drastically change cellulose swelling, as shown in the study by Kasbekar et. al. [25].

3.10. Chemical Resistant:

Pearl millet cellulose showed excellent chemical resistance in both a phosphate buffer solution with a pH of 7.4 and a 0.1 N hydrochloric acid solution, demonstrating that it remains structurally stable in a variety of chemical settings. Phosphate buffer showed less erosion (4.6% reduction), which means that cellulose's strong intermolecular hydrogen bonds and highly crystalline structure make it more stable under physiological settings. On the other hand, 0.1 N HCl showed significantly more erosion (8%), which may be explained by the acid-catalyzed hydrolysis of β-(1→4)-glycosidic links and the weakening of hydrogen bonding in the surrounding cellulose. Surface erosion could be accelerated due to increased oedema and acidic medium penetration. Hydrogels, wound dressings, controlled drug delivery systems, and transdermal patches are just a few examples of the pharmaceutical and biomedical formulations that could benefit from pearl millet cellulose's high chemical stability and durability, as shown by its generally low erosion values. Ershova et al. studied about how cellulose behaves in alkaline environments, both while stabilised and when degrading [26].

3.11. Biodegradability:

Biodegradability of Pearl millet cellulose was assessed by measuring its weight over a period of 21 days. A 13.4% decline was noted, indicating a modest level of natural degradation. In trial that involved burying pearl millet cellulose in mud for 21 days, the weight loss was 13.4%, indicating that it was somewhat biodegradable. The fast degradation of Pearl millet cellulose may be affected by its compact structure and high crystallisation [27].

Table 2 - Characterisation parameters of Pearl Millet cellulose

Parameters	**Result**
Contact Angel (°)	**68.80°**
Moisture content (%)	**105 ± 2°C**
Ash value (%)	**12.0 % ±1.3 %,**
Swelling study (%)	**HCl (0.1 N) - 240%** **pH 7.4 Phosphate buffer- 157.5%** **H2O- 110%**
Chemical resistance (%)	**HCl (0.1 N) - 8%** **pH 7.4 Phosphate buffer- 4.6%**
Biodegradability (%)	**13.4%**

4. CONCLUSION

The agriculture byproducts of pearl millet Showa a significant yet not fully utilised potential as sustainable biomaterial. This research aims to assess the viability of extracting and comprehensively characterising cellulose from pearl millet stalks. Dewaxing, alkali treatment, and bleaching were key processes in the extraction process that effectively extracted refined cellulose by eliminating lignin, hemicellulose, waxes, and other non-cellulosic constituents. Various analytical techniques were employed to characterise the separated cellulose. FTIR examination revealed the presence of characteristic cellulose functional groups and demonstrated the successful removal of non-cellulosic impurities. XRD analysis indicated that the cellulose is crystalline, evidenced by distinct diffraction peaks at 2θ values of around 16°, 22°, and 34°. The results of the TGA and DSC thermal investigations showed that the material had good thermal stability, with almost no deterioration below 300 °C. The SEM examination revealed a rough, porous, and fibrillated surface shape, indicating an increased surface area and enhanced interaction potential. Cellulose showed little degradation in acidic media, pure water, and phosphate buffer solutions, according to chemical resistance experiments. Cellulose swelled considerably in distilled water and very little in acidic and buffered conditions, according to swelling experiments, indicating a high water uptake capacity. The material's eco-friendliness was confirmed by biodegradability testing, which showed slow breakdown over 21 days. By revealing structural changes following biodegradation, FTIR analysis provided additional validation of the degradation process. Cellulose has several desired features, including crystallinity, porosity, thermal stability, hydrophilicity, and biodegradability; the results show that pearl millet agricultural leftovers may be effectively extracted to produce it. Because of these qualities, pearl millet cellulose is a green biomaterial that shows promise for use in packaging, medicine, and pharmaceuticals. This work contributes to the valorisation of agricultural waste by promoting the development of circular bioeconomy approaches that transform renewable biomass into value-added commodities.

ACKNOWLEDGEMENTS

None

AUTHOR CONTRIBUTIONS

Ajesh Chauhan: Writing-Original Draft Preparation, Data Curation, Methodology

Dr. Rishabha Malviya: Supervision, Final Drafting, Conceptualisation, Visualisation.

CONFLICT OF INTEREST

The authors declare that there is no conflict of interest.

ETHICS STATEMENT

Not applicable

DATA AVAILABILITY STATEMENT

Data will be made available on request to the corresponding author

REFERENCES

[1] Dallaev R, Papež N, Allaham MM, Holcman V. Biodegradable polymers: properties, applications, and environmental impact. Polymers. 2025 Jul 18;17(14):1981.

[2] Sajid SA, Tehseen P, Mahmood U, Ghaffar A, Qasim M, Arooj R, Tahir T, Rafique Z. Role of sustainable alternatives to petrochemical based plastics in achieving the SDGs. Indonesian Journal of Agriculture and Environmental Analytics. 2024 Jan;3(1):35-52.

[3] Hira A, Pacini H, Attafuah-Wadee K, Vivas-Eugui D, Saltzberg M, Yeoh TN. Plastic waste mitigation strategies: A review of lessons from developing countries. Journal of Developing Societies. 2022 Sep;38(3):336-59.

[4] Khoaele KK, Gbadeyan OJ, Chunilall V, Sithole B. The devastation of waste plastic on the environment and remediation processes: a critical review. Sustainability. 2023 Mar 15;15(6):5233.

[5] Lithner D, Larsson Å, Dave G. Environmental and health hazard ranking and assessment of plastic polymers based on chemical composition. Science of the total environment. 2011 Aug 15;409(18):3309-24.

[6] Hahladakis JN, Iacovidou E, Gerassimidou S. An overview of the occurrence, fate, and human risks of the bisphenol-A present in plastic materials, components, and products. Integrated environmental assessment and management. 2023 Jan 1;19(1):45-62.

[7] Aggarwal K, Premlata, Mishra S, Kumar R. Recent Preparations and Innovations in the Biodegradable Bioplastics and Biocomposites (A Review). Russian Journal of General Chemistry. 2025 Aug;95(8):1906-23.

[8] Megra MB, Gelaw TB, Worku LA, Pandey DP, Bachheti RK, Bachheti A, Husen A. Bioplastic from Agricultural Waste. InSustainable Solutions for Agricultural Waste (pp. 121-135). CRC Press.

[9] Uesu NY, Pineda EA, Hechenleitner AA. Microcrystalline cellulose from soybean husk: effects of solvent treatments on its properties as acetylsalicylic acid carrier. International journal of pharmaceutics. 2000 Sep 25;206(1-2):85-96.

[10] Sun XF, Sun RC, Su Y, Sun JX. Comparative study of crude and purified cellulose from wheat straw. Journal of agricultural and food chemistry. 2004 Feb 25;52(4):839-47.

[11] Khan MN, Rehman N, Sharif A, Ahmed E, Farooqi ZH, Din MI. Environmentally benign extraction of cellulose from dunchi fiber for nanocellulose fabrication. International Journal of Biological Macromolecules. 2020 Jun 15;153:72-8.

[12] Ahmad A, Khan MN, Rehman N, Kelestemur S, Tariq M, Jan AK, Ahmad S, Eisele DM, Syed W, Al-Rawi MB. Extraction and Characterization of Cellulose and Cellulose Nanocrystals from the Stalks of Marrubium vulgare plant. Carbohydrate Polymer Technologies and Applications. 2025 Jul 15:100947.

[13] Jr JM. Determination of moisture in native and processed cellulose. Industrial & Engineering Chemistry Analytical Edition. 1940 Jul 1;12(7):390-1.

[14] Park YW, Bell LN. Determination of moisture and ash contents of foods. Food Science and Technology-New York-Marcel Dekker-. 2004 Jun 1;138(1):55.

[15] El Seoud OA, Fidale LC, Ruiz N, D'Almeida ML, Frollini E. Cellulose swelling by protic solvents: which properties of the biopolymer and the solvent matter?. Cellulose. 2008 Jun;15(3):371-92.

[16] Singha AS, Thakur VK. Chemical resistance, mechanical and physical properties of biofibers-based polymer composites. Polymer-plastics technology and engineering. 2009 Jun 16;48(7):736-44.

[17] Rumi SS, Liyanage S, Abidi N. Soil burial-induced degradation of cellulose films in a moisture-controlled environment. Scientific Reports. 2024 Mar 22;14(1):6921.

[18] La Mantia FP, Ascione L, Mistretta MC, Rapisarda M, Rizzarelli P. Comparative investigation on the soil burial degradation behaviour of polymer films for agriculture before and after photo-oxidation. Polymers. 2020 Mar 30;12(4):753.

[19] Pavas, Suman, Majumdar AD, Munjal N, Kamboj U. Characterization of Pennisetum Glaucum (Pearl Millet). InJournal of Physics: Conference Series 2022 May 1 (Vol. 2267, No. 1, p. 012020). IOP Publishing.

[20] Costa F, Mendanha D, Gomes JM, Oliveira JA, Ribeiro C, Miranda AF, Barbosa JR, Soares OS, Pereira MF, Santos J, Freitas B. A Comprehensive Study on the Physicochemical Characterisation of Plant-Based By-Products. Materials. 2025 Apr 30;18(9):2054.

[21] Chen QY, Xiao SL, Shi SQ, Cai LP. A one-pot synthesis and characterization of antibacterial silver nanoparticle–cellulose film. Polymers. 2020 Feb 13;12(2):440.

[22] Schellbach SL, Monteiro SN, Drelich JW. A novel method for contact angle measurements on natural fibers. Materials Letters. 2016 Feb 1;164:599-604.

[23] Balasubramanian S, Sharma R, Kaur J, Bhardwaj N. Characterization of modified pearl millet (Pennisetum typhoides) starch. Journal of food science and technology. 2014 Feb;51(2):294-300.

[24] Yadav M, Rengasamy RS, Gupta D. Characterization of pearl millet (Pennisetum glaucum) waste. Carbohydrate polymers. 2019 May 15;212:160-8.

[25] Kasbekar GS, Neale SM. The swelling of cellulose in aqueous solutions of certain acids and salts with measurements of the vapour pressures, densities and viscosities of these solutions. Transactions of the Faraday Society. 1947;43:517-28.

[26] Ershova O, da Costa EV, Fernandes AJ, Domingues MR, Evtuguin DV, Sixta H. Effect of urea on cellulose degradation under conditions of alkaline pulping. Cellulose. 2012 Dec;19(6):2195-204.

[27] Kalka S, Huber T, Steinberg J, Baronian K, Müssig J, Staiger MP. Biodegradability of all-cellulose composite laminates. Composites Part A: Applied Science and Manufacturing. 2014 Apr 1;59:37-44.